# Fermi surface and edge-localized states in graphite studied by high-resolution angle-resolved photoemission spectroscopy

K. Sugawara,[1] T. Sato,[1,2] S. Souma,[1] T. Takahashi,[1,2] and H. Suematsu[3]
[1]*Department of Physics, Tohoku University, Sendai 980-8578, Japan*
[2]*CREST, Japan Science Technology Agency (JST), Kawaguchi 332-0012, Japan*
[3]*Japan Synchrotron Radiation Research Institute, Mikazuki, Hyogo 679-5143, Japan*
(Received 28 June 2005; revised manuscript received 24 October 2005; published 26 January 2006)

We have performed ultrahigh-resolution angle-resolved photoemission spectroscopy on graphite single crystal (kish graphite). We have successfully determined the electronic band structure in the close vicinity of the Fermi level and found an extremely small hole-like Fermi surface centered at the K(H) point. We also found a weakly dispersive band near the Fermi level around the K(H) point, which is not predicted by the bulk band calculation. The origin of this anomalous feature is discussed in relation to the electronic states characteristic of the stepped surfaces.

DOI: 10.1103/PhysRevB.73.045124 PACS number(s): 68.65.−k, 71.20.−b, 79.60.−i, 73.20.At

## I. INTRODUCTION

Carbon-based nanomaterials (nanographite) such as nanotube and fullerene have generated a considerable interest since they show a variety of interesting physical properties such as superconductivity, metal-semiconductor transition, and one-dimensional behavior known as Tomonaga-Luttinger liquid. These anomalous properties owe strongly to the dimensionality, size, and geometry of graphene (single-layer graphite sheet). For example, it has been theoretically suggested[1–5] that a graphite ribbon possesses a characteristic electronic state near the Fermi level ($E_F$) called the edge-localized state. This newly created electronic state at the edge has been intensively discussed in relation to the magnetic and transport properties. It has been theoretically predicted that the magnetic property of graphite ribbon strongly depends on the structure of edge, zigzag, or armchair type,[1,4] and also on the stacking sequence of graphite layers.[6] It is also known that adsorption of hydrogen, oxygen, and fluorine atoms to graphite ribbon remarkably affects and changes the character of edge-localized state.[7,8] Recent STS/STM studies reported a signature of the edge-localized state near $E_F$ in the density of states (DOS).[9] For better understanding of the origin of such anomalous properties of nanographite, it is important to elucidate the basic electronic structure such as the band structure and the Fermi surface (FS) of graphene and/or graphite. Although angle-resolved photoemission spectroscopy (ARPES) has been employed on kish graphite (artificially grown single-crystalline graphite),[10–13] the precise electronic structure in the close vicinity of $E_F$ relevant to the anomalous properties has not been well elucidated because of the limitation of the energy and momentum resolutions.

In this paper, we present ultrahigh-resolution ARPES results on high-quality kish graphite. In addition to the $\pi$ and $\sigma$ bands which are fully consistent with the bulk band calculation, we found an anomalous almost nondispersive band very close to $E_F$. This band is not predicted by the bulk band calculation and appears only in the very small momentum region around the K(H) point in the Brillouin zone, where the highly dispersive $\pi$ band produces a tiny hole pocket. The experimental results are discussed in relation to the edge-localized states and the dangling bond characteristic of the surface.[1–5,14,15]

## II. EXPERIMENTS

Kish graphite is artificially grown single-crystalline graphite produced during purification of iron at high temperatures.[16] The high single-crystalinity of kish graphite used in this study was confirmed by the sharp sixfold x-ray Laue diffraction pattern. ARPES measurements were performed using a GAMMADATA-SCIENTA SES-2002 spectrometer with a high-flux discharge lamp and a toroidal grating monochromator at Tohoku University. We used the He I$\alpha$ ($h\nu$=21.218 eV) and He II$\alpha$ (40.814 eV) resonance lines to excite photoelectrons. The energy and angular resolutions were set at 4–10 meV and 0.2°, respectively. Crystals were cleaved *in situ* in an ultrahigh vacuum of $2\times10^{-11}$ Torr to obtain a clean surface for measurement. The Fermi level ($E_F$) of samples was referred to that of a gold film evaporated onto the sample substrate.

## III. RESULTS AND DISCUSSION

Figure 1(a) shows valence-band ARPES spectra of kish graphite measured at 20 K along the ΓKM (AHL) direction with the He II$\alpha$ resonance line. We clearly find several highly dispersive bands. One band has the top of dispersion at the Γ(A) point at 4 eV and disperses toward the higher binding energy on approaching the K(H) point. This band has the bottom at about 12 eV at the K(H) point and then disperses back toward the lower binding energy on approaching the M(L) point. We also find another prominent peak located at about 8 eV at the Γ(A) point. This band rapidly approaches $E_F$ on moving toward the K(H) point, where the spectrum shows a clear Fermi-edge cutoff indicative of a tiny hole pocket centered at the K(H) point. These features of the overall valence-band structure are consistent with previous ARPES results.[10–13] In order to see more clearly the disper-

 

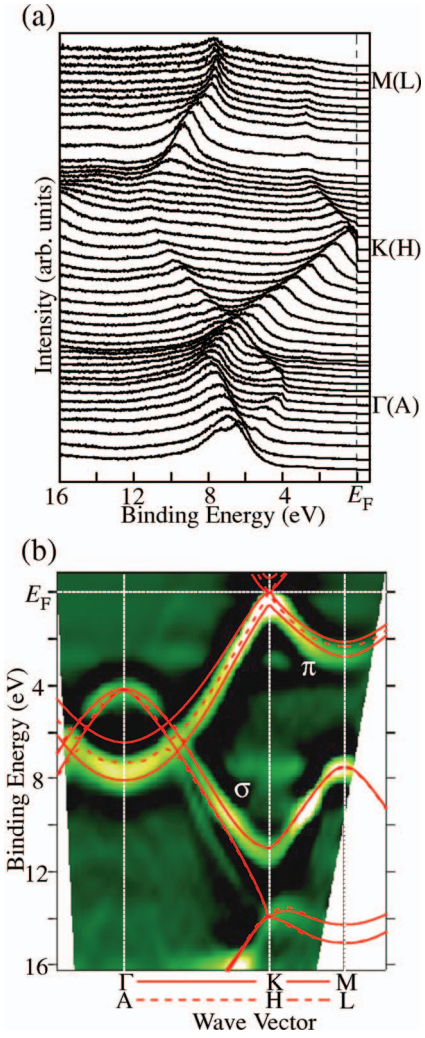


FIG. 1. (Color) (a) ARPES spectra of kish graphite measured at 20 K along the ΓKM direction using He II$\alpha$ resonance line. (b) The experimental band structure of graphite (bright areas) obtained by plotting the second derivative of ARPES-spectral intensity as a function of wave vector and binding energy, compared with the modified first-principles band structure calculation (red lines) (Ref. 17).

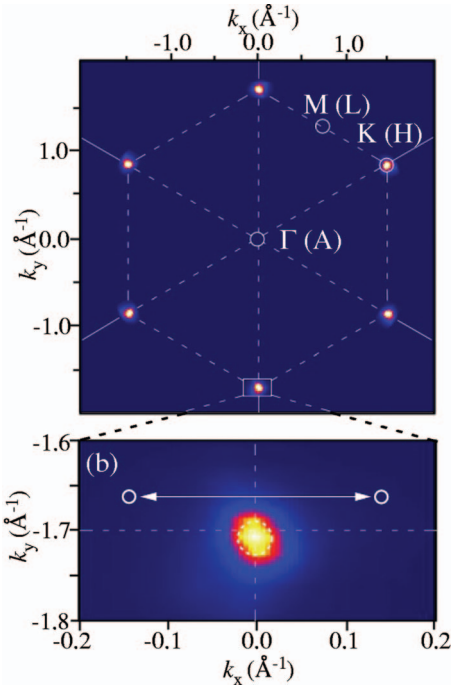


FIG. 2. (Color) (a) The plot of ARPES-spectral intensity at $E_F$ as a function of two-dimensional wave vector, showing the experimental Fermi surface of graphite. Bright area shows the strong intensity. (b) Expansion around the K(H) point. A broken circle at the K(H) point shows the Fermi surface estimated by extrapolating the band dispersion below $E_F$. An arrow indicates the cut where the ARPES measurement shown in Fig. 3 was done.

sive feature of bands in the ARPES spectra, we have mapped out the band structure and show the result in Fig. 1(b). The experimental band structure was obtained by taking the second derivative of ARPES spectra and plotting the intensity by gradual shading as a function of wave vector and binding energy. Bright areas correspond to the experimental bands. Figure 1(b) also shows the first-principle band calculation of graphite[17] using the JD (Johnson and Dresselhaus) model[18] with AB stacking for two high-symmetry lines, ΓKM and AHL. It is clear from the comparison that the overall dispersive feature of bands shows a good agreement between the experiment and the calculation although there are several quantitative differences. For example, the $\sigma$ band due to the C $2p$ bonding states is located at about 4 eV at the Γ(A) point in both the experiment and the calculation, while the dispersive feature from the Γ(A) point to the K(H) point shows a quantitative deviation. The lower-lying branch of the $\sigma$ band is situated at slightly higher binding energy in the experiment than in the calculation. The $\pi$ band is located at a slightly higher binding energy in the experiment than in the calculation at the Γ(A) point, while both perfectly coincide with each other near $E_F$ at the K(H) point in the energy scale of Fig. 1(b).

In order to study the detailed electronic structure near $E_F$ relevant to the observed various anomalous properties, we have performed ARPES measurements with higher energy and momentum resolutions using the He I$\alpha$ resonance line. Figure 2(a) shows the plot of ARPES spectral intensity at $E_F$ as a function of a two-dimensional wave vector. The spectral weight is integrated within 10 meV with respect to $E_F$ and the intensity is plotted by assuming the hexagonal symmetry. The bright area corresponds to the higher intensity. Figure 2(b) shows an expansion around the K(H) point. As clearly seen in Fig. 2, the spectral intensity at $E_F$ is sharply peaked at the K(H) point, demonstrating the existence of an extremely small Fermi surface at the K(H) point, consistent with previous ARPES works.[19–21] It is noted here that Nishimoto *et al.*[19,20] reported that the intensity distribution of photoelectrons near $E_F$ is not even in the first and the second Brillouin zones as well as at the different locations of high symmetry points. In the present experiment, this intensity asymmetry is not seen since we assume the hexagonal symmetry in illustrating Fig. 2. We have estimated the volume of the observed small hole-like Fermi surface as follows. We assumed at first that the hole pocket has an ellipsoidal shape

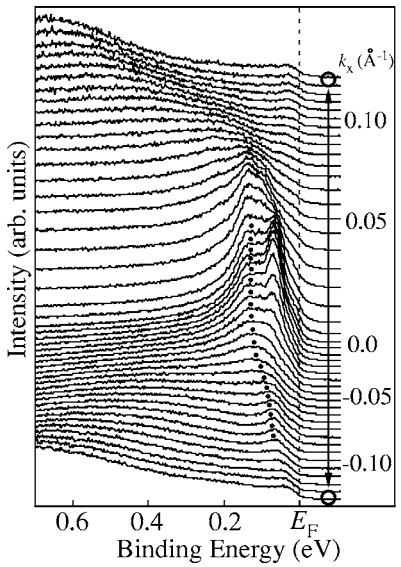


FIG. 3. ARPES spectra in the close vicinity of $E_F$ measured at the cut shown by an arrow in Fig. 2(b). Filled circles show the energy position of peaks.

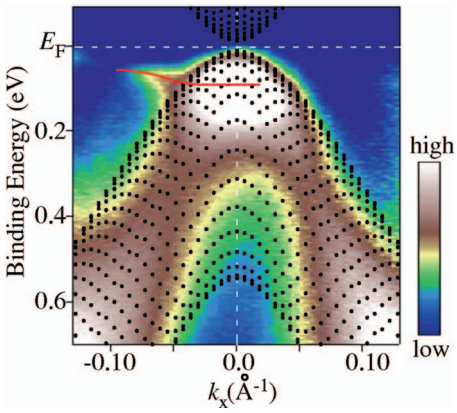


FIG. 4. (Color) The experimental band structure near $E_F$ around the K(H) point obtained by plotting the ARPES-spectral intensity as a function of binding energy and wave vector, compared with the projection of the calculated $\pi$ band onto the (001) plane (small dots) (Ref. 24). The red line shows the peak position of a weakly dispersive band near $E_F$ indicated by filled circles on the spectra in Fig. 3.

elongated along the $k_z$ (KH) axis with a circular cross section in the $k_x$-$k_y$ plane. The longer axis ($2b$) of the ellipsoid is supposed to be a half of the unit cell along the $k_z$ axis, namely the distance between the K and H points, 0.942 Å$^{-1}$, as predicted from the band calculation.[22] We determined the shorter axis ($2a$) of the ellipsoid as $0.034 \pm 0.004$ Å$^{-1}$ by extrapolating the band dispersion near the K(H) point toward $E_F$ with a linear function. The estimated volume ($4\pi a^2 b/3$) of the hole-like Fermi surface is $5.7 \pm 0.7 \times 10^{-4}$ Å$^{-3}$, which corresponds to the carrier number of $9.2 \pm 1.1 \times 10^{18}$ cm$^{-3}$. This value is apparently larger than the hole carrier number ($2.0 \times 10^{18}$) estimated from the Hall coefficient measurement.[23] This difference may be due to the finite energy and momentum resolution in the ARPES measurement.

We found an anomalous feature in the ARPES spectrum near the K(H) point which is not predicted from the bulk band calculation. Figure 3 shows ARPES spectra measured along the cut slightly away from the hole pocket at the K(H) point as shown in Fig. 2(b). We at first notice two prominent structures near $E_F$ around $k_x = 0.0$ Å$^{-1}$. One of them, which is located closer to $E_F$ and forms a sharp peak at about 80 meV, shows a steep dispersion toward high binding energy with rapid broadening of the peak width on going to $k_x = 0.1$ Å$^{-1}$. This band is assigned as the $\pi$ band as described above. It is noted here that this $\pi$ band does not cross or touch $E_F$ since the measurement was done outside of the hole pocket as shown in Fig. 2(b). In addition to the $\pi$ band, we find an anomalous feature (band) at about 130 meV around $k_x = 0.0$ Å$^{-1}$. In contrast to the bulk $\pi$ band, this band shows a peculiar energy dispersion asymmetric with respect to $k_x = 0.0$ Å$^{-1}$. It is almost flat at $k_x = 0.0$ to 0.05 Å$^{-1}$ while it shows a slight upward dispersion toward $E_F$ at $k_x = 0.0$ to $-0.10$ Å$^{-1}$. This asymmetric behavior might be due to the matrix-element effect in the photoelectron exciting process since the polarization of incident light is different between the two cases. We have measured ARPES spectra for several cuts and found that this anomalous feature appears only around the K(H) point. This feature has not been resolved in the previous ARPES experiments[10–13,19–21] possibly due to the insufficient energy and momentum resolution, and the relatively coarse energy/momentum mesh in the ARPES measurements.

In order to elucidate the origin of this anomalous feature near $E_F$, we plot in Fig. 4 the ARPES spectral intensity as a function of binding energy and wave vector, together with the projection of the bulk $\pi$ band onto the (001) plane.[24] As clearly seen in Fig. 4, the projection of the $\pi$ band shows a good agreement with the hole-like $\pi$ band in the experiment. The anomalous feature is observed well outside the projection of the $\pi$ band, indicating that the dispersion along $k_z$ of the $\pi$ band is not responsible for the anomalous feature. The antibonding electron-like $\pi$ band ($\pi^*$ band) might be the origin of the anomalous feature. However, as seen in Fig. 4, the $\pi^*$ band is situated well above $E_F$ in this momentum region and cannot explain the anomalous band below $E_F$. The coupling of electrons with a certain bosonic excitation as observed in cuprate superconductors[25,26] cannot explain this observation because the band produced by such an excitation should follow or mimic the original hole-like dispersion of the $\pi$ band[27] with a considerable renormalization of the bandwidth near $E_F$. However, the observed anomalous band shows an electron-like character in contrast to the hole-like $\pi$ band. The angle-integrated-type background as the origin of the anomalous band is simply denied since such a background structure in ARPES spectrum would show no dispersion contrary to the small but finite energy dispersion of the observed band. The edge-localized state predicted from the calculation for graphite ribbons[1–4] may be one of plausible explanations for the observed anomalous band. According to the recent calculation,[5] a zigzag edge of graphite ribbon possesses an almost-flat band slightly below $E_F$ around the K point in good agreement with the present observation. We speculate that the cleaved surface of kish graphite has similar zigzag edges at the steps. In fact, recent STS/STM studies[9]

reported the existence of zigzag steps and resultant edge-localized states on graphite surface. It has been also revealed that the zigzag step affects the electronic structure substantially away from the step since the edge-localized state is observed on the flat surface about 35 Å away from the step.[9] This long-distant effect of the zigzag step may account for the observation of the edge-localized states by ARPES which probes the electronic structure averaged over a wide area of the surface. Another plausible explanation for the observed anomalous feature is the presence of dangling bonds on the surface.[14,15] It has been theoretically suggested by Jensen and Blase[14] that the character of graphite surface is dramatically affected by the presence of dangling bonds. These dangling bonds are associated to undercoordinated carbon atoms at point or extended defects at the step edges. According to the STM measurement by Hahn and Kang,[15] such dangling bonds which are not passivated by adsorbates contribute to the DOS near $E_F$. We speculate that dangling atoms or dimers at armchair or zigzag edges, which are not passivated by the adosorbates, may be formed in the present experiment where we cleave the sample in an ultrahigh vacuum of $2 \times 10^{-11}$ Torr. In this case, the observed anomalous feature near $E_F$ in the ARPES experiment may be explained by the dangling-bond scenario. Further theoretical and experimental studies to elucidate the anomalous electronic structure at the step edges in graphite are necessary.

## IV. CONCLUSION

We reported ultrahigh-resolution ARPES results on kish graphite. We have determined precisely the band structure and the Fermi surface. In addition to the $\pi$ and $\sigma$ bands which are fully consistent with the bulk band calculation, we found an anomalous almost flat band in the close vicinity of $E_F$ around the K(H) point, which is not predicted from the bulk band calculation or explained in terms of possible intrinsic or extrinsic effects related to the bulk $\pi$ band. We have discussed the origin of this anomalous feature in relation to the electronic states characteristic of the stepped surfaces.

## ACKNOWLEDGMENTS

This work was supported by Grants from JSPS, CREST-JST, and MEXT of Japan. SS thanks JSPS for financial support.

[1] M. Fujita, K. Wakabayashi, K. Nakada, and K. Kusakabe, J. Phys. Soc. Jpn. **65**, 1920 (1996).
[2] K. Nakada, M. Fujita, G. Dresselhaus, and M. S. Dresselhaus, Phys. Rev. B **54**, 17954 (1996).
[3] K. Kobayashi, Phys. Rev. B **48**, 1757 (1993).
[4] K. Wakabayashi, M. Fujita, H. Ajiki, and M. Sigrist, Phys. Rev. B **59**, 8271 (1999).
[5] K. Sasaki, S. Murakami, and R. Saito, cond-mat/0508442.
[6] Y. Miyamoto, K. Nakada, and M. Fujita, Phys. Rev. B **59**, 9858 (1999).
[7] M. Maruyama and K. Kusakabe, J. Phys. Soc. Jpn. **73**, 656 (2004).
[8] M. Maruyama, K. Kusakabe, S. Tsuneyuki, K. Akagi, Y. Yoshimoto, and J. Ymauchi, J. Phys. Chem. Solids **65**, 119 (2004).
[9] T. Matsui, H. Kambara, Y. Niimi, K. Tagami, M. Tsukada, and H. Fukuyama, Phys. Rev. Lett. **94**, 226403 (2005).
[10] T. Takahashi, H. Tokailin, and T. Sagawa, Phys. Rev. B **32**, 8317 (1985).
[11] A. R. Law, M. T. Johnson, and H. P. Hughes, Phys. Rev. B **34**, 4289 (1986).
[12] A. Santoni, J. J. Terminello, F. J. Himpsel, and T. Takahashi, Appl. Phys. A **A52**, 299 (1991).
[13] T. Kihlgren, T. Balasubramanian, L. Wallden, and R. Yakimova, Phys. Rev. B **66**, 235422 (2002).
[14] P. Jensen and X. Blase, Phys. Rev. B **70**, 165402 (2004).
[15] J. R. Hahn and H. Kang, Phys. Rev. B **60**, 6007 (1999).
[16] N. Joshima, M. Koyama, H. Yoshida, S. Matsuo, and H. Nagasaki, Proc. Int. Conf. Carbon, edited by M. Igarashi (1982), p. 523.
[17] R. C. Tatar and S. Rabii, Phys. Rev. B **25**, 4126 (1982).
[18] L. G. Johnson and G. Dresselhaus, Phys. Rev. B **7**, 2275 (1973).
[19] T. Matsushita, H. Nishimoto, T. Okuda, T. Nakatani, H. Daimon, S. Suga, H. Namba, T. Ohta, Y. Kagoshima, and T. Miyahara, J. Electron Spectrosc. Relat. Phenom. **78**, 489 (1996).
[20] H. Nishimoto, T. Okuda, T. Nakatani, H. Daimon, T. Matsushita, S. Imada, and S. Suga, Solid State Commun. **98**, 671 (1996).
[21] F. Matsui, Y. Hori, H. Miyata, N. Suganuma, H. Daimon, H. Totsuka, K. Ogawa, T. Furukubo, and H. Namba, Appl. Phys. Lett. **81**, 2556 (2002).
[22] J.-C. Charlier, J. P. Michenaud, X. Gonze, and J.-P. Vigneron, Phys. Rev. B **44**, 13237 (1991).
[23] N. B. Brandt, S. M. Chudinov, and Y. G. Ponomarev, *Graphite and Its Compounds, Semimetals Vol. 20.1* (North-Holland, Amsterdam, 1988).
[24] J. W. Mclcure, Phys. Rev. **108**, 612 (1957).
[25] A. Lanzara, P. V. Bogdanov, X. J. Zhou, S. A. Kellar, D. L. Feng, E. D. Lu, T. Yoshida, H. Eisaki, A. Fujimori, K. Kishio, J.-I. Shimoyama, T. Noda, S. Uchida, Z. Hussain, and Z.-X. Shen, Nature (London) **412**, 510 (2001).
[26] J. C. Campuzano, H. Ding, M. R. Norman, H. M. Fretwell, M. Randeria, A. Kaminski, J. Mesot, T. Takeuchi, T. Sato, T. Yokoya, T. Takahashi, T. Mochiku, K. Kadowaki, P. Guptasarma, D. G. Hinks, Z. Konstantinovic, Z. Z. Li, and H. Raffy, Phys. Rev. Lett. **83**, 3709 (1999).
[27] M. R. Norman, H. Ding, J. C. Campuzano, T. Takeuchi, M. Randeria, T. Yokoya, T. Takahashi, T. Mochiku, and K. Kadowaki, Phys. Rev. Lett. **79**, 3506 (1997).